In the case of enolsilanes, the initial equilibrium is not as favorable. Thus, retro-Michael reaction competes with desilylation of B, and the observed stereoselectivity is a result of either partial or complete thermodynamic control. With these compounds, we suggest that anti stereochemistry predominates because gauche interactions are minimized in conformation F, relative to G (Scheme III). This hypothesis nicely explains the observed anti stereoselectivity and the fact that stereoselectivity is largely independent of enol silane stereostructure.

Acknowledgment. This work was supported by a research grant from the United States Public Health Service (AI15027).

Registry No. 1, 89043-59-4; **2**, 89043-58-3; **3**, 51425-54-8; **4**, 19980-41-7; **5**, 61878-68-0; **6**, 66323-99-7; **7**, 95740-73-1; **8**, 72658-08-3; **9**, 51425-53-7; **10**, 19980-42-8; **11**, 71268-59-2; **12**, 72658-15-2; $TiCl_4$, 7550-45-0; $SnCl_4$, 7646-78-8; *t*-BuC(O)CH=CHMe, 20971-19-1; *t*-BuC(O)CH=CHPr-*i*, 38343-04-3; *t*-BuC(O)CH=CHPh, 29569-91-3; MeC(O)CH=CHMe, 3102-33-8; R′C(O)CH=CHR″ (R′, R″= $(CH_2)_3$), 930-68-7; *i*-PrC(O)CH=CHMe, 50396-90-2; EtC(O)CH=CHMe, 50396-87-7; PhC(O)CH=CHMe, 35845-66-0; *t*-BuC(O)CH=CHEt, 38343-01-0; *t*-BuC(O)CH=CHBu-*t*, 20859-13-6; *t*-BuOC(O)CH(Me)CH(Me)CH_2C(O)Bu-*t* (isomer 1), 95740-74-2; *t*-BuOC(O)CH(Me)CH(Me)CH_2C(O)Bu-*t* (isomer 2), 95740-75-3; *t*-BuOC(O)CH(Me)CH(*i*-Pr)CH_2C(O)Bu-*t* (isomer 1), 95740-76-4; *t*-BuOC(O)CH(Me)CH(*i*-Pr)CH_2C(O)Bu-*t* (isomer 2), 95740-77-5; *t*-BuOC(O)CH(Me)CH(Ph)CH_2C(O)Bu-*t* (isomer 1), 95740-78-6; *t*-BuOC(O)CH(Me)CH(Ph)CH_2C(O)Bu-*t* (isomer 2), 95740-79-7; *t*-BuOC(O)CH(Me)CH(Me)CH_2C(O)Me (isomer 1), 95740-80-0; *t*-BuOC(O)CH(Me)CH(Me)CH_2C(O)Me (isomer 2), 95740-81-1; *t*-BuOC(O)CH(Me)CH(R″)CH_2C(O)R′ (R′,R″ = $(CH_2)_3$) (isomer 1), 95740-83-3; *t*-BuOC(O)CH(Me)CH(R″)CH_2C(O)R′ (R′,R″ = $(CH_2)_3$) (isomer 2), 95740-84-4; EtC(O)CH(Me)CH(Me)CH_2C(O)Bu-*t* (isomer 1), 95740-85-5; EtC(O)CH(Me)CH(Me)CH_2C(O)Bu-*t* (isomer 2), 95740-86-6; EtC(O)CH(Me)CH(Me)CH_2C(O)Pr-*i* (isomer 1), 95740-87-7; EtC(O)CH(Me)CH(Me)CH_2C(O)Pr-*i* (isomer 2), 95740-88-8; *i*-PrC(O)CH(Me)CH(Me)CH_2C(O)Et (isomer 1), 95740-89-9; *i*-PrC(O)CH(Me)CH(Me)CH_2C(O)Et (isomer 2), 95740-90-2; *i*-PrC(O)CH(Me)CH(Me)CH_2C(O)Pr-*i* (isomer 1), 95740-91-3; *i*-PrC(O)CH(Me)CH(Me)CH_2C(O)Pr-*i* (isomer 2), 95740-92-4; *i*-PrC(O)CH(Me)CH(Me)CH_2C(O)Bu-*t* (isomer 1), 95740-93-5; *i*-PrC(O)CH(Me)CH(Me)CH_2C(O)Bu-*t* (isomer 2), 95740-94-6; *i*-PrC(O)CH(Me)CH(Me)CH_2C(O)Ph (isomer 1), 95740-95-7; *i*-PrC(O)CH(Me)CH(Me)CH_2C(O)Ph (isomer 2), 95740-96-8; *i*-PrC(O)CH(Me)CH(Et)CH_2C(O)Bu-*t* (isomer 1), 95740-97-9; *i*-PrC(O)CH(Me)CH(Et)CH_2C(O)Bu-*t* (isomer 2), 95740-98-0; *i*-PrC(O)CH(Me)CH(*i*-Pr)CH_2C(O)Bu-*t* (isomer 1), 95740-99-1; *i*-PrC(O)CH(Me)CH(*i*-Pr)CH_2C(O)Bu-*t* (isomer 2), 95741-00-7; *i*-PrC(O)CH(Me)CH(Ph)CH_2C(O)Bu-*t* (isomer 1), 95741-01-8; *i*-PrC(O)CH(Me)CH(Ph)CH_2C(O)Bu-*t* (isomer 2), 95741-02-9; *t*-BuC(O)CH(Me)CH(Me)CH_2C(O)Pr-*i* (isomer 1), 95741-03-0; *t*-BuC(O)CH(Me)CH(Me)CH_2C(O)Pr-*i* (isomer 2), 95741-04-1; *t*-BuC(O)CH(Me)CH(Me)CH_2C(O)Bu-*t* (isomer 1), 95741-05-2; *t*-BuC(O)CH(Me)CH(Me)CH_2C(O)Bu-*t* (isomer 2), 95741-06-3; PhC(O)CH(Me)CH(Me)CH_2C(O)Pr-*i* (isomer 1), 95741-07-4; PhC(O)CH(Me)CH(Me)CH_2C(O)Pr-*i* (isomer 2), 95741-08-5; PhC(O)CH(Me)CH_2C(O)Bu-*t* (isomer 1), 95741-09-6; PhC(O)CH(Me)CH(Me)CH_2C(O)Bu-*t* (isomer 2), 95741-10-9; PhC(O)CH(Me)CH(Me)CH_2C(O)Ph (isomer 1), 95741-11-0; PhC(O)CH(Me)CH(Me)CH_2C(O)Ph (isomer 2), 95741-12-1; PhC(O)CH(Me)CH(Et)CH_2C(O)Bu-*t* (isomer 1), 95741-13-2; PhC(O)CH(Me)CH(Et)CH_2C(O)Bu-*t* (isomer 2), 95741-14-3; PhC(O)CH(Me)CH(*i*-Pr)CH_2C(O)Bu-*t* (isomer 1), 95741-15-4; PhC(O)CH(Me)CH(*i*-Pr)CH_2C(O)Bu-*t* (isomer 2), 95741-16-5; PhC(O)CH(Me)CH(Ph)CH_2C(O)Bu-*t* (isomer 1), 95741-17-6; PhC(O)CH(Me)CH(Ph)CH_2C(O)Bu-*t* (isomer 2), 95741-18-7; *p*-$MeOC_6H_4$C(O)CH(Me)CH(Me)C(O)Bu-*t* (isomer 1), 95741-19-8; *p*-$MeOC_6H_4$C(O)CH(Me)CH(Me)C(O)Bu-*t* (isomer 2), 95741-20-1; 2,4,6-$Me_3C_6H_4$C(O)CH(Me)CH(Me)C(O)Bu-*t* (isomer 1), 95741-21-2; 2,4,6-$Me_3C_6H_4$C(O)CH(Me)CH(Me)C(O)Bu-*t* (isomer 2), 95741-22-3; *t*-$BuMe_2SiOC(O)CH(Me)CH(Me)CH_2C(O)Bu$-*t* (isomer 1), 95741-23-4; *t*-$BuMe_2SiOC(O)CH(Me)CH(Me)CH_2C(O)Bu$-*t* (isomer 2), 95741-24-5; *t*-$BuMe_2SiOC(O)CH(Me)CH(i\text{-}Pr)CH_2C(O)Bu$-*t* (isomer 1), 95741-25-6; *t*-$BuMe_2SiOC(O)CH(Me)CH(i\text{-}Pr)CH_2C(O)Bu$-*t* (isomer 2), 95741-26-7; *t*-$BuMe_2SiOC(O)CH(Me)CH(Ph)CH_2C(O)Bu$-*t* (isomer 1), 95741-27-8; *t*-$BuMe_2SiOC(O)CH(Me)CH(Ph)CH_2C(O)Bu$-*t* (isomer 2), 95741-28-9; *t*-$BuMe_2SiOC(O)CH(Me)CH(Me)CH_2C(O)Me$ (isomer 1), 95741-29-0; *t*-$BuMe_2SiOC(O)CH(Me)CH(Me)CH_2C(O)Me$ (isomer 2), 95740-82-2; *t*-$BuMe_2SiOC(O)CH(Me)CH(R'')CH_2C(O)R'$(R′,R″ = $(CH_2)_3$) (isomer 1), 95741-30-3; *t*-$BuMe_2SiOC(O)CH(Me)CH(R'')CH_2C(O)R'$(R′,R″ = $(CH_2)_3$) (isomer 2), 95741-31-4.

Supplementary Material Available: Methods used to assign stereostructures and ^{13}C NMR chemical shifts of the products of the reactions summarized in Table I (4 pages). Ordering information is given on any current masthead page.

Geometrical Isomers of a Bridgehead Imine: (*E*)- and (*Z*)-2-Azabicyclo[3.2.1]oct-1-ene and 2-Azabicyclo[2.2.2]oct-1-ene

Juliusz G. Radziszewski,[1a] John W. Downing,[1a] Curt Wentrup,[1a,b] Piotr Kaszynski,[1a] Mikolaj Jawdosiuk,[1c] Peter Kovacic,[1c] and Josef Michl*[1a,d]

Departments of Chemistry, University of Utah Salt Lake City, Utah 844112 University of Wisconsin, Milwaukee, Wisconsin 53201

Received October 29, 1984

Irradiation of matrix-isolated bridgehead azides yields highly strained bridgehead imines.[2-6] 1-Azidonorbornane (**1**) would be expected to provide access to both 2-azabicyclo[3.2.1]oct-1-ene (**2**) and 2-azabicyclo[2.2.2]oct-1-ene (**3**), but only the IR of the

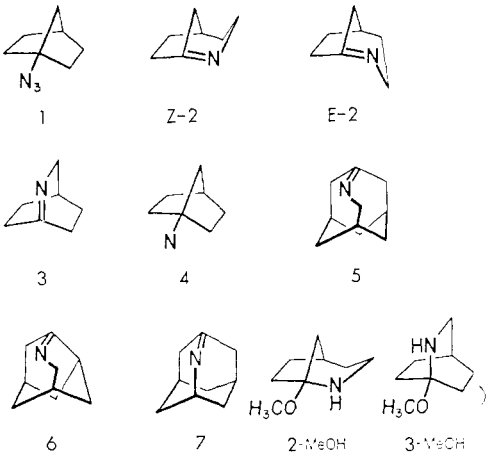

former was detected in recently reported matrix-isolation work and assigned to the less strained *Z* form.[4] Our results for matrix-isolated **1**, obtained by using monochromatic irradiation, IR, UV, and ESR spectroscopy and trapping with methanol, show that the situation is considerably more complicated: (*E*)-**2**, (*Z*)-**2**, **3**, and **4** are all formed, and (*E*)-**2** can be photoisomerized to (*Z*)-**2**.

UV irradiation[7a,b] of **1** isolated in Ar or polyethylene matrices at 12 K causes a gradual disappearance of its characteristic UV and IR absorption spectra[8] and a gradual growth of new peaks,

(1) (a) University of Utah. (b) On sabbatical leave from University of Marburg, Marburg, Germany. (c) University of Wisconsin, Milwaukee. (d) Presented at the 187th National ACS Meeting, St. Louis, MO, April 1984.

(2) Michl, J.; Radziszewski, J. G.; Downing, J. W.: Wiberg, K. B.; Walker, F. H.; Miller, R. D.; Kovacic, P.; Jawdosiuk, M.; Bonačič-Koutecký, V. *Pure Appl. Chem.* **1983**, *55*, 315.

(3) Dunkin, I. R.; Shields, C. J.; Quast, H.; Seiferling, B. *Tetrahedron Lett.* **1983**, *24*, 3887.

(4) Sheridan, R. S.; Ganzer, G. A. *J. Am. Chem. Soc.* **1983**, *105*, 6158.

(5) Radziszewski, J. G.; Downing, J. W.; Wentrup, C.; Kaszynski, P.; Jawdosiuk, M.; Kovacic, P.; Michl, J. *J. Am. Chem. Soc.* **1985**, *107*, 594–603.

(6) Radziszewski, J. G.; Downing, J. W.; Jawdosiuk, M.; Kovacic, P.; Michl, J. *J. Am. Chem. Soc.* **1985**, *107*, 594.

(7) Irradiations were performed (a) at 308 nm by using a Lambda Physik XeCl excimer laser, (b) at 310 ± 15 nm by using a 2500-W high-pressure Xe–Hg lamp and an interference filter protected by a broad-band $NiSO_4/H_2O$ filter, (c) at 415 nm by using a Coherent krypton ion laser, (d) at $\lambda > 365$ nm by using a cutoff filter and a 200-W high-pressure Hg lamp, (e) at 254 nm by using a low-pressure Hg lamp;

(8) UV of **1** (polyethylene, 12 K) 222, 287 nm; (Ar, 12 K) 287 nm. IR of **1** (Ar, 12 K) 2103 (asym str), 1271 (sym str), 727 and 467 (bend) cm^{-1}. [3-^{15}N]-1-Azidonorbornane (49 atom % ^{15}N) was prepared according to the method given in ref 5 and had IR (neat, room temperature) 2099, 1237, 714, and 457 cm^{-1}.

0002-7863/85/1507-2799$01.50/0

Table I. Observed and Computed Properties of Imines

	3	(*E*)-2	(*Z*)-2	$(CH_3)_2C{=}NCH_3$
$\tilde{\nu}_{C=^{14}N}$(exptl), cm^{-1}	1481	1475	1586/82	1669[a]
$\tilde{\nu}_{C=^{14}N}$(calcd),[b] cm^{-1}	1493	1523	1591	(1669)
$\tilde{\nu}_{C=^{15}N}$(exptl), cm^{-1}	1462		1566/63	
$\tilde{\nu}_{C=^{15}N}$(calcd),[b] cm^{-1}	1474	1503	1569	
$\tilde{\nu}$("nπ*")(exptl),[c] 10^3 cm^{-1}	~25 (w)	~25 (w)	33.6 (w)	41.7[d] (~200)
$\tilde{\nu}$("nπ*")(calcd),[e] 10^3 cm^{-1}	20.3 (0.05)	19.5 (0.04)	28.9 (0.04)	30.0 (0.01)
$\tilde{\nu}$("ππ*")(exptl),[c] 10^3 cm^{-1}	42.2 (m)	~42 (w)	49.5 (s)	~55[d] (~10000)
$\tilde{\nu}$("ππ*")(calcd),[e] 10^3 cm^{-1}	35.4 (0.06)	37.9 (0.10)	43.9 (0.2)	56.4 (0.4)
C=N bond length,[b] Å	1.33	1.32	1.31	1.29
pyramidalization at C,[b,f] deg	12	13	13	0
C=N—C angle,[b] deg	108	112	113	126
torsion angle,[b,g] deg	69	74	39	0
charge on C,[b,h] |e|	0.041	0.051	0.012	0.022
charge on N,[b] |e|	−0.307	−0.321	−0.251	−0.285
dipole moment,[b] *D*	1.06	1.00	1.10	0.99
$\Delta H_f°$,[b] kcal/mol	66.2	70.1	45.4	0.5

[a] Dunkin, I. R.; Thompson, P. C. P. *Tetrahedron Lett.* **1980**, *21*, 3813. [b] MNDO geometry optimization and force field calculations. The calculated IR frequencies were corrected using a scaling factor of 0.854, obtained[6] by fitting the experimental value for *N*-methyl-2-propanimine. [c] Peak maxima; extinction coefficient or relative strength in parentheses. [d] Sandorfy, C. In "The Chemistry of the Carbon–Nitrogen Double Bond"; Patai, S., Ed.; Interscience: London, 1970; p 38. [e] INDO/S vertical excitation energies at ground-state MNDO equilibrium geometries. [f] Defined as $\theta - 90°$, where θ is the magnitude of the three equal angles between the three bonds originating in the imine carbon and an axis chosen to pass through it. [g] Defined as the dihedral angle between the planes defined by the C=N bond and (i) the axis described under *f* and (ii) the N—C bond. [h] Double-bonded carbon.

associated with four products: (i) the already reported[4] colorless one assigned as (*Z*)-**2**, stable to visible radiation[7c,d] and destroyed very slowly at 254[7e] or 308 nm,[7a,b,9] (ii) a first orange one assigned as (*E*)-**2**, and (iii) a second orange one assigned as **3**.[10] These two colored products are formed in relative proportions which depend on the irradiation conditions; the highest observed ratio of (*E*)-**2** to (*Z*)-**2** was about 1:20. The former is extremely sensitive to visible and particularly to UV light, which converts it to (*Z*)-**2**. The latter is transformed slowly by visible or 308-nm light or rapidly by 254-nm light into a product characterized by IR and UV, whose structure is still under investigation: (iv) an ESR-active one, assigned as **4**, insensitive to visible light, destroyed fairly rapidly at 308 nm and slowly at 254 nm. This is present in trace amounts even under conditions that are optimal for its formation (254-nm irradiation of **1**) and we have not observed it by IR.

All four products are stable in the matrix in the dark and are destroyed upon matrix warm-up. Their individual spectra were extracted by taking advantage of their wavelength-selective response to light (Table I, Figure 1).

The visible spectra of (*E*)-**2** and **3** are very similar, as are their C=N stretching frequencies. The assignment of the (*E*)-**2** structure to one of the orange products is based on its easy photoisomerization to (*Z*)-**2**, which has close precedent in the photoresolution of 4-azahomoadamant-3-ene (**5**).[6]

The structures **2** and **3** were distinguished by trapping experiments. Irradiation of **1** in a room-temperature solution containing methanol yields a mixture of methanol adducts, **2**–MeOH and **3**–MeOH, expected from **2** and **3**.[11] In a methanol-doped argon matrix, the spectra of the primary photoproducts are still observed, with minor shifts. Warm-up yields two major products, regardless of whether the species assigned as (*Z*)-**2**, (*E*)-**2**, and **3** were all present or whether (*E*)-**2** was first photoconverted to (*Z*)-**2**. Capillary GC (SE 52, 40 m) and ^1H NMR comparisons with authentic samples establish their identity as **2**–MeOH and **3**–MeOH. When both orange products are fully bleached with visible light before the warm-up, GC analysis reveals that **2**–MeOH is still produced but **3**–MeOH no longer is. If this bleaching is not carried to completion, reduced amounts of **3**–MeOH relative to **2**–MeOH result upon warm-up.

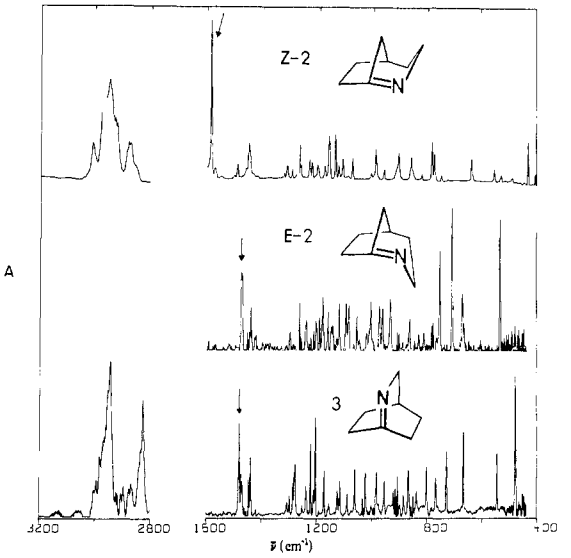

Figure 1. IR spectra at (*Z*)-**2**, (*E*)-**2**, and **3** isolated in Ar matrix (12 K). The arrows indicate C=N stretching bands. The spectra in polyethylene are virtually identical. The weaker peaks in the spectrum of (*E*)-**2** may be due to noise, but the 20 or so most intense ones are reproducible.

The structure assignments are further supported by the observed spectral properties. The spectra of (*Z*)-**2** are quite close to those of 4-azaprotoadamant-3-ene (**6**) ("nπ*" 31900, "ππ*" 49000 cm^{-1}; $\tilde{\nu}_{C=N}$ 1591 cm^{-1})[5] and 4-azahomoadamant-3-ene (**5**) ("nπ*" 33100, "ππ*" 46700 cm^{-1}; $\tilde{\nu}_{C=N}$ 1600 cm^{-1});[6] all three contain a trans double bond in a seven-membered ring. The spectra of (*E*)-**2** and **3** correspond to a higher degree of torsion but still lower than in 2-azaadamant-1-ene (**7**) ("nπ*" 20200, "ππ*" 39700 cm^{-1}; $\tilde{\nu}_{C=N}$ 1451 cm^{-1});[5] these three imines contain a trans double bond in a six-membered ring. The $\tilde{\nu}_{C=N}$ assignments are based on ^{15}N isotopic shifts (Table I; cf. 19 cm^{-1} in **7**[5] and 18 cm^{-1} in **5**[6] and in **6**[5]).

The $\tilde{\nu}_{C=N}$ frequencies and isotopic shifts for the presently reported imines generally agree well with MNDO[12] force field calculations, only the calculated $\tilde{\nu}_{C=N}$ frequency for (*E*)-**2** being much too high (Table I). This enhances the credibility of the MNDO equilibrium geometries also characterized in Table I. The

(9) The previously reported[4] photostability of this material to UV irradiation was undoubtedly due to the use of a weaker light source. The product has been characterized by IR and UV spectra and its structure is under examination.

(10) These products escaped observation previously, presumably since they were destroyed by the $\lambda > 270$ nm light used.[4]

(11) Reed, J. O.; Lwowski, W. *J. Org. Chem.* **1971**, *36*, 2864.

(12) Dewar, M. J. S.; Thiel, W. *J. Am. Chem. Soc.* **1977**, *99*, 4899, 4907. Dewar, M. J. S.; Ford, G. P.; McKee, M. L.; Rzepa, H. S.; Thiel, W.; Yamaguchi, Y. *J. Mol. Struct.* **1978**, *43*, 135.

"$n\pi^*$" and "$\pi\pi^*$" excitation energies calculated by the INDO/S method[13] at these geometries (Table I) reflect the experimental trends correctly but are a little too low, as was also the case for other imines.[5,6]

The structure assignment of the nitrene **4** is based on its ESR signal at 0.8124 T (9.3 GHz; assuming $E = 0$, $|D/hc| = 1.65$ cm^{-1}),[14] a sharp UV peak at 33 560 cm^{-1}, whose intensity follows that of the ESR signal,[15] and on photochemical trapping with CO in Ar at 36 K. The IR spectrum of this matrix, containing **2**, **3**, CO, and presumably **4**, was unchanged for many hours in the dark, but on UV irradiation[7c] a weak band of 1-norbornyl isocyanate at 2263 cm^{-1} appeared[16] (IR, MS, and GC comparison with an authentic sample).

To our knowledge, the above results represent the first observation of geometrical isomerism at a strained bridgehead double bond. Taken together with prior work,[2-6] they suggest that the C=N stretching frequencies are typically reduced by about 100 cm^{-1} in *trans*-azacycloheptene rings and by about 200 cm^{-1} in *trans*-azacyclohexene rings, respectively, relative to an unstrained imine.

Acknowledgment. This work was supported by the National Science Foundation (CHE 81-21122).

Registry No. **1**, 65864-91-7; (*E*)-**2**, 95673-67-9; (*Z*)-**2**, 95673-68-0; **3**, 95673-69-1; **4**, 95673-70-4.

(13) Ridley, J.; Zerner, M. *Theor. Chim. Acta* **1973**, *32*, 111.
(14) Wasserman, E.; Snyder, L. C.; Yager, W. A. *J. Chem. Phys.* **1964**, *41*, 1763; Wasserman, E. *Prog. Phys. Org. Chem.* **1971**, *8*, 319.
(15) This can be compared with the energy of the 0–0 band of fluorescence of methylnitrene triplet in the gas phase, 31 806 cm^{-1}: Carrick, P. G.; Engelking, P. C. *J. Chem. Phys.* **1984**, *81*, 1661.
(16) For precedent see: Dunkin, I. R.; Thompson, P. C. P. *J. Chem. Soc., Chem. Commun.* **1982**, 1192 and ref 6.

Mixed-Valence $Mn^{II}Mn^{III}$ Complexes: Models for the Manganese Site in the Photosynthetic Electron-Transport Chain

Bouchra Mabad,[1a] Jean-Pierre Tuchagues,*[1a]
Yeong Tsyr Hwang,[1b] and David N. Hendrickson*[1b]

Laboratoire de Chimie de Coordination du CNRS associé à l'Université Paul Sabatier 31400 Toulouse, France
School of Chemical Sciences, University of Illinois Urbana, Illinois 61801
Received July 5, 1984

Two or four manganese ions serve as the active site for oxygen evolution in the photosynthetic electron-transport chain.[2] Recently two research groups[3] independently reported an EPR signal for the S_2 oxidation state of this manganese site, and, on the basis of the magnitude of observed hyperfine structure, they attributed the signal to a binuclear $Mn^{III}Mn^{IV}$ site[3] or a tetranuclear $Mn_3^{III}Mn^{IV}$ site.[4] The limited number of mixed-valence manganese complexes needs to be increased to characterize better the EPR signal for the S_2 state.

The complexes Mn^{II}(saldien) and Mn^{II}[5-NO_2(saldien)],[5,6] where saldien and 5-NO_2(saldien), respectively, result from the Schiff base condensation of diethylenetriamine and either salicylaldehyde or 5-nitrosalicylaldehyde, have proven to be useful precursors to new mixed-valence manganese complexes. A solution of either of these complexes when allowed to react with O_2 and then frozen gives a 16-hyperfine-line EPR spectrum as is illustrated in Figure 1A for Mn^{II}[5-NO_2(saldien)] in a DMF–toluene glass at 120 K. This EPR spectrum looks like the spectrum reported[7] for frozen glasses of the $Mn^{III}Mn^{IV}$ complex

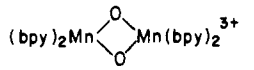

However, as indicated below, the mixed-valence complexes derived from O_2 oxidation of Mn^{II}(saldien) and Mn^{II}[5-NO_2(saldien)] are $Mn^{II}Mn^{III}$ complexes. A caveat concerning the identification of manganese oxidation states based on magnitudes of hyperfine interactions is advanced in this paper.

The time development of the O_2 oxidation of the two saldien Mn^{II} complexes under strictly anhydrous conditions was monitored with EPR. The rate of O_2 oxidation of Mn^{II}[5-NO_2(saldien)] in solution is slow in comparison to Mn^{II}(saldien). In the case of the former complex dissolved in $C_2H_4Cl_2$, within a few minutes of exposure to dry oxygen, a 16-line EPR spectrum for a frozen solution is readily visible superimposed on a very broad, wide ranging Mn^{II} spectrum.[3] If the solution is warmed to room temperature for periods of time, then refrozen, the intensity of the 16-line spectrum grows slowly at the expense of the Mn^{II} spectrum. A double integration of the whole 7000 G X-band spectrum as a function of time shows a continuous decrease in the total EPR signal. After 120 h, the intensity of the total EPR signal remains constant at $\sim^1/_{10}$ of that of the initial Mn^{II} complex whose wide-ranging spectrum has totally disappeared. During this reaction, the yellow orange solution turns slowly brown-green and a green powder precipitates very slowly. EPR spectra run for the green powders exhibit a temperature dependence. At room temperature, the signal is characterized by several fine structure resonances spread out over 5000 G. As the sample temperature is decreased, the $g = 2$ resonance grows at the expense of the other

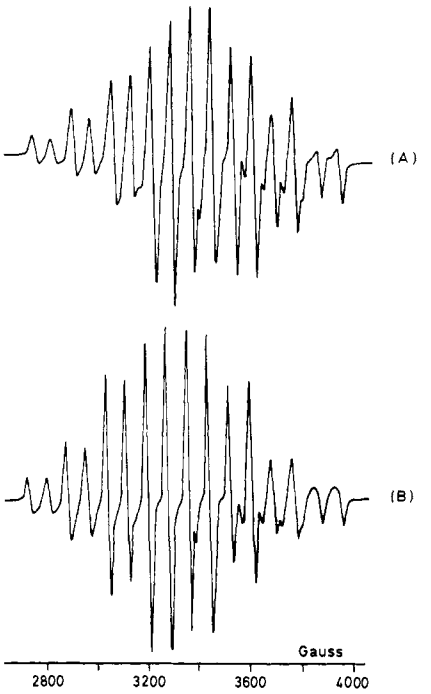

Figure 1. X-band EPR spectrum (A) for the oxygenation product of Mn^{II}[5-NO_2(saldien)] in frozen DMF–toluene glass at 120 K (63 mW and field modulation of 10 G). Trace (B) illustrates the simulated spectrum obtained with the parameters and approach[11] described in the text.

(1) (a) CNRS and Université Paul Sabatier. (b) University of Illinois.
(2) (a) Amesz, J. *Biochim. Biophys. Acta* **1983**, *726*, 1–12. (b) Livorness, J.; Smith, T. D. *Struct. Bonding (Berlin)* **1982**, *48*, 2–44. (c) Sauer, K. *Acc. Chem. Res.* **1980**, *13*, 249–256. (d) Radmer, R.; Cheniae, G. In "Topics in Photosynthesis"; Barber, J., Ed.; Elsevier: Amsterdam, 1977.
(3) (a) Dismukes, G. C.; Siderer, Y. *Proc. Natl. Acad. Sci. U.S.A.* **1981**, *78*, 274–278. (b) Hansson, Ö.; Andreasson, L. E. *Biochim. Biophys. Acta* **1982**, *679*, 261–268.
(4) Dismukes, G. C.; Ferris, K.; Watnick, P. *Photobiochem. Photobiophys.* **1982**, *3*, 243–256.
(5) Coleman, W. M.; Boggess, R. K.; Hughes, J. W.; Taylor, L. T. *Inorg. Chem.* **1981**, *20*, 700–706.
(6) Mabad, B.; Tuchagues, J. P.; Hwang, Y. T.; Hendrickson, D. N., unpublished results.
(7) Cooper, S. R.; Dismukes, G. C.; Klein, M. P.; Calvin, M. *J. Am. Chem. Soc.* **1978**, *100*, 7248–7252.

0002-7863/85/1507-2801$01.50/0